Level velocity statistics of hyperbolic chaos

R. Sankaranarayanan *

Physical Research Laboratory,
Navrangpura, Ahmedabad 380009, India.

Abstract

A generalized version of standard map is quantized as a model of quantum chaos. It is shown that, in hyperbolic chaotic regime, second moment of quantum level velocity is $\sim 1/\hbar$ as predicted by the random matrix theory.

* Present Address: Center for Nonlinear Dynamics, Department of Physics, Bharathidasan University, Trichy 620024, India.

I. INTRODUCTION

Chaotic systems are characterized by positive lyapunov exponents such that in phase space neighbourhood trajectories diverge exponentially. Among the chaotic systems there are special class of systems which are *completely* chaotic or hyperbolic [1]. Phase space of hyperbolic systems has only unstable orbits as there are expanding and contracting real directions with positive and negative lyapunov exponents respectively. Area preserving maps like cat map and baker map are examples of hyperbolic systems. Even the well known standard map of kicked rotor, a text book paradigm of Hamiltonian chaos [2], is not proven to be hyperbolic even for strong external kick strength.

In the study of chaotic quantum systems, it is of fundamental interest to characterize highly chaotic (but not known to be hyperbolic) and hyperbolic chaotic regimes in quantum domain. This forms our motivation here, and to pursue further it would be more appropriate to quantize a *single* dynamical system which has parameters for highly chaotic *and* hyperbolic chaotic regimes. In one of our earlier works, a generalized version of standard map was introduced to study the dynamics of a kicked particle trapped inside an one dimensional infinite square well potential [3]. The generalization, arising from length scales namely well width and field wave length, has parameters to fulfill the present requirement. With our knowledge, there is no other single system possessing parameters for the above mentioned classical regimes.

In quantum domain, dynamics of levels in parameter space is known to have manifestations of classical complexity. While quantum levels cross each other for regular case, they exhibit avoided crossings when underlying classical dynamics is chaotic. Level dynamics can be described by level velocity wherein system parameter plays the role of pseudo-time. In Ref. [4] the notion of curvature i.e., second derivative of levels with parameter, is introduced to quantify the avoided crossings. It is known that the curvature distribution of chaotic system follows an universal behaviour [5].

In this connection, one another quantity of importance is the second moment of level velocity. A semiclassical analysis of kicked system shows that second moment is the sum of all classical time correlations of the kicking potential, such that lowest (zeroth) order correlation being the Random Matrix Theory (RMT) predicted second moment [6]. It is also known for quantized standard map that, in highly chaotic regime there are systematic deviations between second moment and the corresponding RMT prediction. The deviations are thus related to the non-vanishing higher order classical time correlations [6].

In the present work, we introduce quantum version of a generalized standard map as a model of quantum chaos to study the level velocity statistics. In particular, we compute the second moment and compare with the RMT prediction in order to characterize different chaotic regimes.

II. THE MODEL

A. Classical system

Considering a particle trapped in a one dimensional infinite square well potential $V_0(q)$ of unit width (hard walls at $q = \pm 1/2$), which experiences a periodic kick from an external pulsed field. The Hamiltonian is

$$\tilde{H} = \frac{p^2}{2} + V_0(q) + \frac{k\lambda}{4\pi^2}\cos\left(\frac{2\pi q}{\lambda}\right)\sum_j \delta(j-t) \tag{1}$$

and underlying kick to kick dynamics of the particle is *equivalent* to discrete dynamics described by a dimensionless area-preserving mapping:

$$\begin{aligned} p_{j+1} &= p_j + \frac{k}{2\pi}\sin(2\pi r q_j) \\ q_{j+1} &= q_j + p_{j+1} \end{aligned} \tag{2}$$

which is defined on 2-torus i.e., a unit square $[-1/2, 1/2) \times [-1/2, 1/2)$ with periodic boundaries. Here $r = 1/\lambda$ is ratio of two length scales of the system namely, well width and field wavelength; k is effective strength of the kick. This is the *Generalized Standard Map* (GSM) which was introduced in our earlier studies on the above Hamiltonian [3].

GSM is continuous when r is integer and discontinuous otherwise. One can immediately recognize that widely studied standard map of kicked rotor is a special case ($r = 1$) of GSM. Since the standard map is a continuous map, for small ($k < 1$) dynamics is predominantly regular wherein many rotational invariant circles (also called as KAM tori) are interspersed in the phase space. They act as forbidden barriers for chaotic orbits to diffuse. Gradual destruction of these invariant structures with the increase of k, leads to onset of chaos; for $k \gg 1$, dynamics is highly chaotic. On the other hand, when r is non-integer no KAM tori exist in the phase space. In this case, depends of the parameter r the phase space is either mixed or fully chaotic even for small k values.

The Jacobian $\mathbf{J}$ of GSM is such that

$$|\text{Trace } \mathbf{J}| = |2 + kr\cos(2\pi r q_j)|\,. \tag{3}$$

Since $|q_j| \leq 1/2$, for $r \leq 1/2$ $|\text{Trace } \mathbf{J}| > 2$. That is to say Jacobian has real eigenvalues. In other words, the system is *completely* chaotic or hyperbolic for $r \leq 1/2$. In this regime there are contracting and expanding real directions or alternatively stable and unstable manifolds throughout the phase space. Thus GSM is realized as a rare class of dynamical system as it has parameters for both highly chaotic and hyperbolic chaotic regimes.

B. Quantum system

GSM arises from the equation of motion of free particle in presence of a field $V(q)$ which is applied as time periodic impulse. The field is defined as: $V(q) = k\cos(2\pi r q)/(4\pi^2 r)$; $V(q) = V(q+1)$ and the Hamiltonian is

$$H = \frac{p^2}{2} + V(q)\sum_j \delta(j-t)\,. \tag{4}$$

By integrating Shrödinger equation over unit time we obtain corresponding quantum propagator as

$$\hat{U} = e^{-i\hat{p}^2/2\hbar}\;\; e^{-iV(\hat{q})/\hbar}\,. \tag{5}$$

Then the quantum dynamics can be described as $|\psi(t+1)\rangle = \hat{U}|\psi(t)\rangle$, which is a quantum analogue of the classical map.

On quantizing 2-torus phase space by introducing periodic boundary conditions both in q and p [7] we have: $\hat{q}|n\rangle = (n/N)|n\rangle$; $\hat{p}|m\rangle = (m/N)|m\rangle$ where $n, m = -N/2, -N/2 + 1 \ldots N/2 - 1$. Here $N = (2\pi\hbar)^{-1}$ is the dimensionality of the Hilbert space and the semi-classical limit is $N \to \infty$. The position and momentum eigenstates obey the periodicity $|n+N\rangle = |n\rangle$; $|m+N\rangle = |m\rangle$ and the transformation function is

$$\langle n|m\rangle = \frac{1}{\sqrt{N}} \exp\left[\frac{i2\pi mn}{N}\right] . \tag{6}$$

Being a homogeneous linear system, Shrödinger equation in finite N dimensional space has solutions $|\phi_j\rangle$, $j = 1, 2, \ldots N$, which are linearly independent. Since the Hamiltonian is time periodic (unit period), according to Floquet theory [8] the solutions satisfy eigenvalue equation $\hat{U}|\phi_j\rangle = e^{-i\phi_j}|\phi_j\rangle$. Eigenstates $|\phi_j\rangle$ are quasienergy states and eigenangles ϕ_j are quasienergies. Then general solution at a given time is $|\psi\rangle = \sum_j c_j|\phi_j\rangle$ where c_j are constants. As a consequence of hermiticity of Hamiltonian, quasienergy states are orthogonal and they form a complete set in finite N dimensional space.

Matrix form of the propagator in discrete position representation is [9]

$$U_{nn'} \equiv \langle n|\hat{U}|n'\rangle = \frac{1}{\sqrt{N}} \exp\left[-i\pi\left\{\frac{1}{4} - \frac{(n-n')^2}{N} + 2NV\left(\frac{n'}{N}\right)\right\}\right] . \tag{7}$$

The Hamiltonian (4) has reflection symmetry about the origin i.e., $H(q,p) = H(-q,-p)$. This symmetry is reflected in the quantum propagator matrix

$$U_{nn'} = \frac{e^{-i\pi/4}}{\sqrt{N}}\, e^{i\pi(n-n')^2/N} \exp\left\{\frac{-ikN}{2\pi r} \cos\left[\frac{2\pi r}{N}(n'+\alpha)\right]\right\} \tag{8}$$

through the relation $[\hat{U}, \hat{R}] = 0$ where the hermitian operator $\hat{R}$ is defined as

$$\begin{aligned} \hat{R}|n\rangle &= |-n\rangle \qquad \text{for } \alpha = 0 \\ &= |-n-1\rangle \quad \text{for } \alpha = 0.5\,. \end{aligned} \tag{9}$$

Note that a phase factor α is introduced in the matrix element to avoid exact quantum symmetry. Since $\hat{R}^2 = 1$ we may label the eigenstates of $\hat{U}$ with eigenvalues ± 1 of $\hat{R}$ i.e., the states are $|\phi_\pm\rangle$. For $\alpha = 0.5$, symmetry matrix of order N is

$$R_N = \langle n|\hat{R}|n'\rangle = \delta(n + n' + 1) \pmod N \tag{10}$$

which has ones along secondary diagonal and zeros elsewhere. Then the state components have a relation $\langle -n-1|\phi\rangle = \pm\langle n|\phi\rangle$ i.e.,

$$|\phi_\pm\rangle = \begin{pmatrix} |v\rangle \\ \pm R_{N/2}|v\rangle \end{pmatrix} . \tag{11}$$

Eigenstates can be numerically obtained by diagonalizing the matrix $U_{nn'}$ of order N. If N is even integer, there are $N/2$ even parity states $\{|\phi_+\rangle\}$ and $N/2$ odd parity states $\{|\phi_-\rangle\}$. On exploiting R-symmetry, the diagonalization can be reduced to the matrix of order $N/2$ by standard procedure [10]. The reduced matrix is

$$\mathcal{U}_{nn'} = \frac{e^{-i\pi/4}}{\sqrt{N}} \exp\left\{\frac{-ikN}{2\pi r}\cos\left[\frac{2\pi r}{N}\left(n+\frac{1}{2}-\frac{N}{2}\right)\right]\right\} \times \left\{e^{i\pi(n-n')^2/N} \pm e^{i\pi(n+n'+1)^2/N}\right\} \quad (12)$$

where $n, n' = 0, 1, \ldots N/2-1$. Now the separation of parity states is obvious.

III. SPECTRAL STATISTICS

One of the standard statistical measures for a chaotic quantum system is the nearest neighbour spacing distribution of quantum levels. For a regular system, levels are clustered such that the spacings follow Poisson distribution. On the other hand, in chaotic case the levels exhibit repulsion such that spacings exhibit RMT predicted Wigner distribution. We expect the classical complexity of GSM, arises due to the parameter r, will also have manifestation in the spectral spacings. It is evident from Fig. 1 that, in contrast to the predominantly regular case, for $r = 0.5$ (hyperbolic) the spacings follow Wigner distribution.

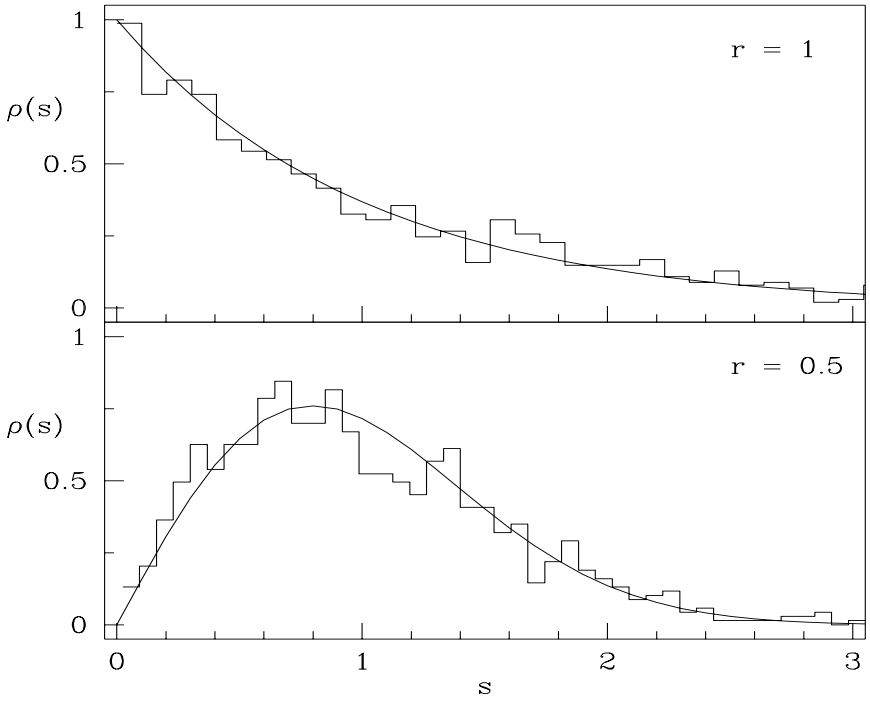

FIG. 1: Nearest neighbour spacing distributions of 1000 quasienergies which correspond to even parity states for $k = 0.3$ with $\alpha = 0.5$. Smooth curves are the Poisson and Wigner distribution.

A. Level velocities

Having seen the effect of r in the spectral spacing, we further investigate on dynamics of the quasienergies in parameter space i.e., level velocities. To be specific, we study second moments of level velocities in different classical regimes. We take $\alpha = 0.35$ so that R-symmetry is broken in the quantum system, and the factor α is dropped out in following expressions for the sake of convenience. Quasienergies $\phi_j \equiv \phi_j(k, r)$ have scaled velocities:

$$\begin{aligned} x_j &= \left(\frac{2\pi^2 r^2}{N}\right) \frac{\partial \phi_j}{\partial k} \\ &= \left(\frac{2\pi^2 r^2}{N}\right) \left[\frac{1}{\hbar}\langle\phi_j|\partial V/\partial k|\phi_j\rangle\right] \\ &= \pi r \sum_n \cos(2\pi r n/N)|\langle n|\phi_j\rangle|^2 \end{aligned} \tag{13}$$

and

$$\begin{aligned} y_j &= \left(\frac{2\pi r^2}{Nk}\right) \frac{\partial \phi_j}{\partial r} \\ &= \left(\frac{2\pi r^2}{Nk}\right) \left[\frac{1}{\hbar}\langle\phi_j|\partial V/\partial r|\phi_j\rangle\right] \\ &= -2\pi r \sum_n (n/N)\sin(2\pi r n/N)|\langle n|\phi_j\rangle|^2 - \sum_n \cos(2\pi r n/N)|\langle n|\phi_j\rangle|^2. \end{aligned} \tag{14}$$

Average velocities in semiclassical limit are

$$\begin{aligned} \langle x\rangle &= \frac{1}{N}\sum_j x_j = \sin(\pi r) \\ \langle y\rangle &= \frac{1}{N}\sum_j y_j = \cos(\pi r) - \frac{2\sin(\pi r)}{\pi r}\,. \end{aligned} \tag{15}$$

Then the second moment of x is given by

$$\begin{aligned} \langle x^2\rangle &= \frac{1}{N}\sum_j x_j^2 \\ &= (\pi r)^2 \left\{ \sum_n \cos^2(2\pi r n/N) \left\langle |\langle n|\phi_j\rangle|^4 \right\rangle \right. \\ &\qquad \left. + \sum_{n\neq n'} \cos(2\pi r n/N)\cos(2\pi r n'/N) \left\langle |\langle n|\phi_j\rangle|^2 |\langle n'|\phi_j\rangle|^2 \right\rangle \right\} \end{aligned} \tag{16}$$

Assuming that spectral averaged eigenfunction components are independent of specific position eigenvalues n, terms within the angle brackets can be taken out of the sum. Then

$$\langle x^2\rangle \sim (\pi r)^2 \left\{ \left[\left\langle |\langle n|\phi_j\rangle|^4 \right\rangle - \left\langle |\langle n|\phi_j\rangle|^2 |\langle n'|\phi_j\rangle|^2 \right\rangle \right] \sum_n \cos^2(2\pi r n/N) + \left\langle |\langle n|\phi_j\rangle|^2 |\langle n'|\phi_j\rangle|^2 \right\rangle \left[\sum_n \cos(2\pi r n/N) \right]^2 \right\} . \tag{17}$$

In chaotic regimes, standard RMT results [11]

$$\begin{aligned} \left\langle |\langle n|\phi_j\rangle|^4 \right\rangle &= 3[N(N+2)]^{-1} \simeq 3N^{-2} \\ \left\langle |\langle n|\phi_j\rangle|^2 |\langle n'|\phi_j\rangle|^2 \right\rangle &= [N(N+2)]^{-1} \simeq N^{-2} \end{aligned} \tag{18}$$

which correspond to Gaussian orthogonal ensemble are applicable here as well. It should be noted that application of RMT results essentially adopt the assumption made above. Replacing the sum by integration in semiclassical limit we arrive to

$$\langle x^2\rangle_{\rm RMT} = \frac{(\pi r)^2}{N} \left[1 + \frac{\sin(2\pi r)}{2\pi r} \right] + \langle x\rangle^2 . \tag{19}$$

Similarly the second moment of y is

$$\langle y^2\rangle = \frac{1}{N} \sum_j y_j^2 \tag{20}$$

$$\begin{aligned} &= \sum_n \{ [2\pi r (n/N) \sin(2\pi r n/N)]^2 + \cos^2(2\pi r n/N) \\ &\quad + 4\pi r (n/N) \sin(2\pi r n/N) \cos(2\pi r n/N) \} \left\langle |\langle n|\phi_j\rangle|^4 \right\rangle \\ &\quad + \sum_{n\neq n'} \{ (2\pi r/N)^2 n n' \sin(2\pi r n/N) \sin(2\pi r n'/N) + \cos(2\pi r n/N) \cos(2\pi r n'/N) \\ &\quad + 4\pi r (n/N) \sin(2\pi r n/N) \cos(2\pi r n'/N) \} \left\langle |\langle n|\phi_j\rangle|^2 |\langle n'|\phi_j\rangle|^2 \right\rangle \end{aligned} \tag{21}$$

and the RMT prediction is

$$\langle y^2\rangle_{\rm RMT} = \frac{1}{N} \left\{ 1 + \frac{(\pi r)^2}{3} + \frac{\sin(2\pi r)}{2\pi r} \left[\frac{5}{2} - (\pi r)^2 \right] - \frac{3}{2} \cos(2\pi r) \right\} + \langle y\rangle^2 . \tag{22}$$

In chaotic regime, quantum states are such that the quantities in left hand side of Eqn. (18) fluctuate about the respective RMT values. These fluctuations could lead to the failure of RMT in predicting the second moment. In Ref. [6] a semiclassical analysis on the systematic deviation between the second moment and its RMT prediction has been made. Here we are interested to see the validity of the RMT prediction in different classical regimes. For that we define normalized deviations:

$$\Delta_x = \left| \frac{\langle x^2 \rangle - \langle x^2 \rangle_{\rm RMT}}{\langle x^2 \rangle} \right| \;\; ; \;\; \Delta_y = \left| \frac{\langle y^2 \rangle - \langle y^2 \rangle_{\rm RMT}}{\langle y^2 \rangle} \right| \tag{23}$$

and taking average of the two positive quantities as

$$\Delta = \frac{\Delta_x + \Delta_y}{2} \, . \tag{24}$$

The deviation is calculated for various parameters and plotted in Fig. 2. Let us first consider the data obtained for small values of k (0.3 and 0.1). As we see the deviation is nearly zero for $r \leq 1/2$. For further values of r, the deviation is found to be significantly large. This is expected as the underlying classical dynamics is predominantly regular or mixed and the RMT is not applicable. On the other hand, the data for large k (5 and 25) exhibit different behaviour. Though the classical phase space is highly chaotic for these parameters, significant deviation observed for various values of r shows the failure of RMT prediction. However, it is noticable from the four sets of observation that for $r \leq 1/2$ the deviation is nearly zero.

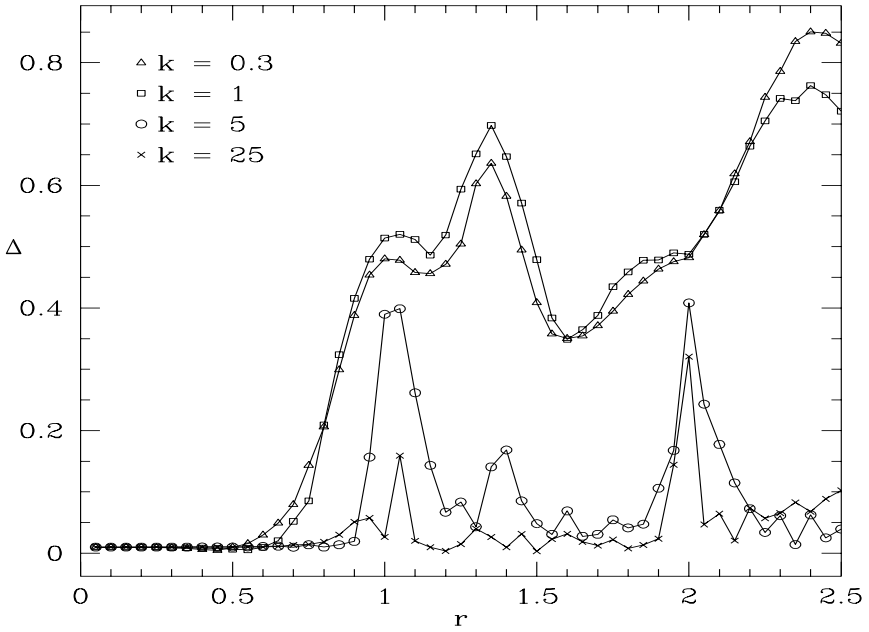

FIG. 2: Deviation between level velocity second moments and RMT predictions. In all the cases we have taken $\alpha = 0.35$ and $N = 200$.

In Fig. 3, the deviation is plotted for two cases by varying k. For $r = 1$ the deviation has strong fluctuations with k. The large deviation for $k < 5$ is due to the predominantly regular/mixed behaviour of the underlying classical system. We also observe significant deviation when k is close to integer multiples of 2π. This may be attributed to the presence of "accelerator modes" [12], which are small regular regions embedded in the sea of chaotic phase space. On the other hand, for $r = 0.5$ the deviation remains negligible irrespective of k values. This shows that RMT predicts second moment of level velocity in hyperbolic chaotic regime. From the Eqn. (19), we see that $\langle x^2 \rangle_{\rm RMT} \sim 1/N$ or $\langle (\partial\phi/\partial k)^2 \rangle_{\rm RMT} \sim N \sim 1/\hbar$. We obtain the same result for the velocity with respect to r as well.

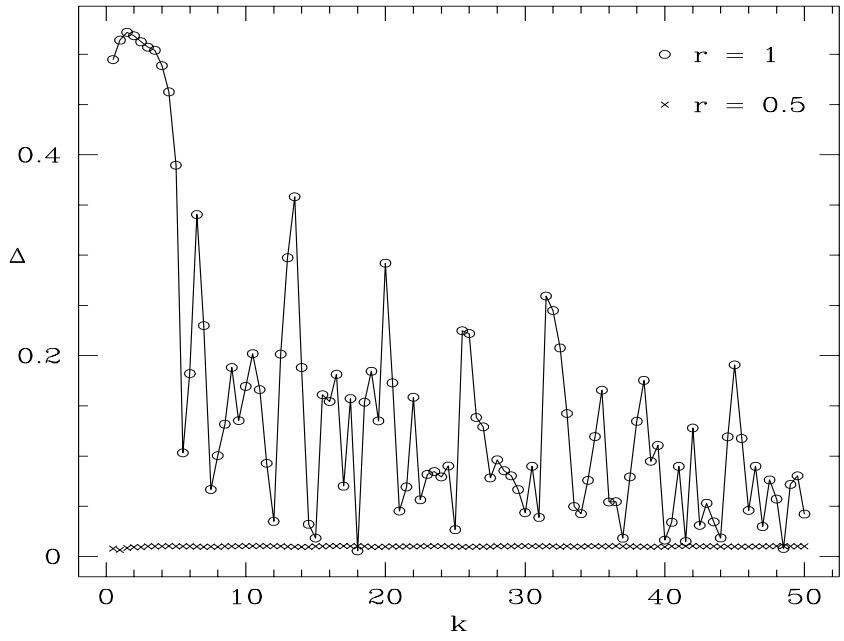

FIG. 3: Deviation between level velocity second moments and RMT predictions. We have taken $\alpha = 0.35$ and $N = 200$.

B. Sawtooth map

In this section we study another quantum model whose classical counterpart has hyperbolic regime. Consider a free particle that is subjected to a time periodic impulsive potential $V(q) = -\lambda q^2/2; V(q+1) = V(q)$. Kick to kick dynamics of such a particle is described by the sawtooth map [13]:

$$\begin{aligned} p_{j+1} &= p_j + \lambda q_j \\ q_{j+1} &= q_j + p_{j+1} \end{aligned} \tag{25}$$

defined on a unit torus. This map is stable for $-4 < \lambda < 0$ and unstable (or hyperbolic) otherwise. Quantized version of this map can be obtained, as usual, upon introducing periodic boundaries in q and p. Details of quantized sawtooth map are given elsewhere [14]. Note that here also the earlier symmetry arguments hold. From the corresponding quasienergies and quasienergy states, we define the scaled level velocity as

$$z_j = \left(\frac{-1}{N\pi}\right)\frac{d\phi_j}{d\lambda} = -2\left\langle \phi_j \left| \frac{dV}{d\lambda} \right| \phi_j \right\rangle = \sum_n (n/N)^2 |\langle n|\phi_j\rangle|^2 \tag{26}$$

with average $\langle z \rangle = 1/12$. Then the second moment is given by

$$\langle z^2 \rangle = \frac{1}{N}\sum_j z_j^2 = \sum_n (n/N)^4 \left\langle |\langle n|\phi_j\rangle|^4 \right\rangle + \sum_{n\neq n'} (n/N)^2 (n'/N)^2 \left\langle |\langle n|\phi_j\rangle|^2 |\langle n'|\phi_j\rangle|^2 \right\rangle . \tag{27}$$

Repeating the earlier procedures, we find the RMT prediction as

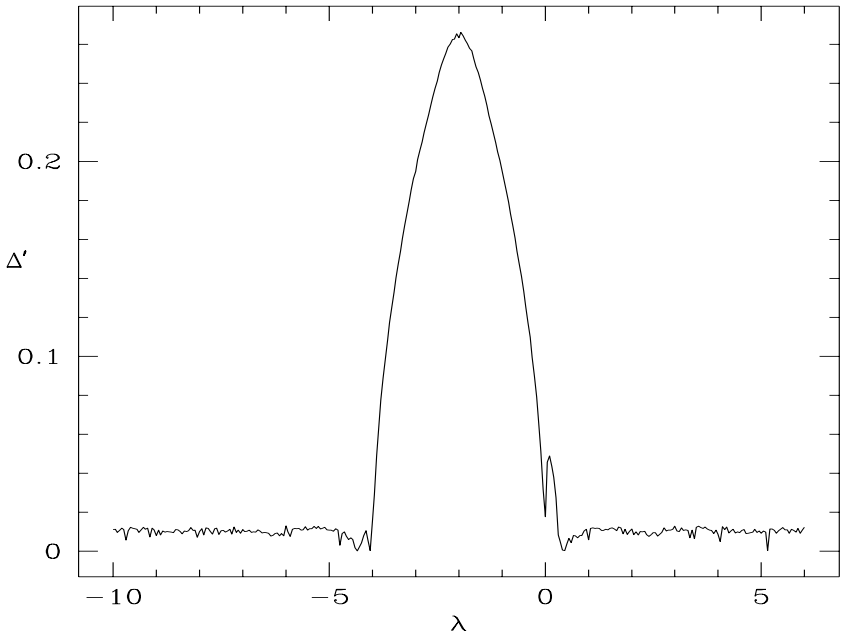

FIG. 4: Deviation Δ' for the quantum sawtooth map with $\alpha = 0.35$ and $N = 200$.

$$\langle z^2 \rangle_{\rm RMT} = \frac{1}{40N} + \langle z \rangle^2 . \tag{28}$$

Defining normalized deviation as

$$\Delta' = \left| \frac{\langle z^2 \rangle - \langle z^2 \rangle_{\rm RMT}}{\langle z^2 \rangle} \right| \tag{29}$$

in Fig. 4 we have plotted the deviation for different λ values. In the stable region $-4 < \lambda < 0$, where the RMT result is not applicable, the deviation is large. Evidently, RMT predicts level velocity second moment in hyperbolic regime. Eqn. (28) shows that $\langle z^2 \rangle_{\rm RMT} \sim 1/N$ or $\langle (d\phi/d\lambda)^2 \rangle_{\rm RMT} \sim N \sim 1/\hbar$. Here also we see that second moment is inversely proportional to the Planck constant for hyperbolic chaos.

IV. CONCLUSION

In this paper we have introduced quantum version of a generalized standard map. The classical system corresponds to the dynamics of a particle, trapped in an 1D infinite square well potential, in presence of time-periodic kicks. For different classical regimes, the second moment of quantum level velocity is computed and compared with the RMT prediction. We have shown that while the prediction fails in highly chaotic regime, the second moment is well predicted by the RMT as $\sim 1/\hbar$ in hyperbolic chaotic regime. By considering another example viz., quantum sawtooth map, the RMT prediction of second moment in hyperbolic chaotic regime has been reinforced. We hope the presented result would shed new lights to explore more on quantum hyperbolic chaos.

Acknowledgement

The author is greatful to Dr. A. Lakshminarayan for useful discussions.

---

[1] Edward Ott, Chaos in Dynamical Systems, Cambridge University Press, 1993.
[2] A.J. Lichtenberg and M.A. Lieberman, Regular and Chaotic Dynamics, Springer-Verlag, 1992.
[3] R. Sankaranarayanan, A. Lakshminarayan, and V.B. Sheorey, Phys. Lett. A 279 (2001) 313.
[4] P. Gaspard, S.A. Rice, and K. Nakamura, Phys. Rev. Lett. 63 (1989) 930; P. Gaspard, S.A. Rice, H.J. Mikeska and K. Nakamura, Phys. Rev. A 42 (1990) 4015.
[5] D. Saher and F. Haake, Phys. Rev. A 44 (1991) 7481; T. Takami and H. Hasegawa, Phys. Rev. Lett. 68 (1992) 419; J. Zakrzewski and D. Delande, Phys. Rev. E 47 (1993) 1650.
[6] A. Lakshminarayan, N.R. Cerruti and S. Tomsovic, Phys. Rev. E 60 (1999) 3992.
[7] J. Ford, G. Mantica and G.H. Ristow, Physica D 50 (1991) 493.
[8] D.W. Jordan and P. Smith, Nonlinear Ordinary Differential Equations, Oxford, 1977.
[9] A. Lakshminarayan, Pramana J. Phys. 48 (1997) 517.
[10] M. Saraceno, Ann. Phys. (N.Y.) 190 (1989) 1.
[11] T.A. Brody, J. Flores, J.B. French, P.A. Mello, A. Pandey and S.S.M. Wong, Rev. Mod. Phys. 53 (1981) 385.
[12] G.M. Zaslavsky, M. Edelman and B.A. Niyazov, Chaos 7 (1997) 159.
[13] John R. Cary and James D. Meiss, Phys. Rev. A 24 (1981) 2664.
[14] A. Lakshminarayan and N.L. Balazs, Chaos Solitons & Fractals 5 (7) (1995) 1169.